

Measurements of the two-dimensional energy spectra of wall-turbulence at high Reynolds number

J. P. Monty, D. Chandran, R. Baidya, and I. Marusic

Department of Mechanical Engineering
The University of Melbourne, Victoria 3010, Australia
email: montyjp@unimelb.edu.au

ABSTRACT

This paper describes a technique to experimentally measure the two-dimensional energy spectra of the streamwise velocity in wall-turbulence. The technique is validated at low Reynolds numbers using Direct Numerical Simulation (DNS) data. It is found that a correction to the high wavenumber range of the energy spectra is required owing to physical limitations on minimum probe separation. The measurement technique and DNS-based correction scheme is employed in the University of Melbourne High Reynolds number (Re) wind-tunnel to measure the 2D spectra at high Re for the first time. The results are compared with attached eddy simulation models, showing that hierarchies of high-aspect ratio eddies are required to accurately capture the large-scale energy behaviour.

INTRODUCTION

Obtaining multi-dimensional statistical turbulence quantities at high Reynolds number is a notoriously difficult problem. Direct Numerical Simulation (DNS) removes the difficulty of multiple dimensions, but does not yet reach the high Reynolds numbers of wind-tunnel facilities. Most analysis of high Reynolds number turbulence data is limited to single-point measurements (or a small number of points of data). This constrains data analysis and can lead to misunderstanding of important flow behaviours. An example is the energy spectra; almost all spectra available at high Reynolds number ($Re_\tau > 10000$) is one-dimensional. A common observation from these data is a lack of evidence for self-similarity of the inertial scales (Nickels *et al.*, 2005; Rosenberg *et al.*, 2013). However, Davidson *et al.* (2006) highlighted that the 1-D energy spectra might not be an ideal tool to observe self-similarity. Their work suggested that aliasing could contaminate the 1-D streamwise spectra by artificially shifting the energy to lower wavenumbers. A 2-D spectrum details the contribution of both the streamwise ($\lambda_x = 2\pi/k_x$, where k_x is the streamwise wavenumber) and spanwise ($\lambda_y = 2\pi/k_y$, where k_y is the spanwise wavenumber) length scales to the total turbulent intensity, but it is not easily obtained experimentally. Another way to describe the problem with the 1-D spectrum is that it is a line integral of a 2-D spectrum and does not reveal any information along the direction of integration. For example, a 1-D streamwise spectrum only provides the energy contribution by a particular streamwise length scale, λ_x , and does not inform us of the range of λ_y associated with that particular λ_x . This leads to the aforementioned aliasing in 1-D spectra. The 2-D spectrum is devoid of such aliasing errors. Here we demonstrate a method to measure the 2-D spectrum in a wind-tunnel boundary layer.

This study is partly motivated by recent work by the authors: from dimensional considerations, Chung *et al.* (2015) argued that, in order to have a k_x^{-1} behaviour in the 1-D spectrum, a region of constant energy in the 2-D spectrum should be bounded by

$\lambda_y/z \sim f_1(\lambda_x/z)$ and $\lambda_y/z \sim f_2(\lambda_x/z)$ where f_1 and f_2 are identical power laws. At low Reynolds number, Del Alamo *et al.* reported that such a region of constant energy is bounded at larger scales by a square-root relationship of the form $\lambda_y/z \sim (\lambda_x/z)^{1/2}$. The attached eddy hypothesis of Townsend (1976) was considered, where hierarchies of geometrically self-similar eddies (whose lengths scale with z) suggest a region in the 2-D spectra at high Reynolds numbers to be bounded by a linear relationship, $\lambda_y \sim \lambda_x$. Here we will examine the first measured 2-D spectra of wall-turbulence at high Reynolds number in the search for evidence for or against self-similarity in the large-scales.

It should be noted that, throughout this study, x , y and z denotes the streamwise, spanwise and wall-normal directions respectively and u , v and w denotes the corresponding velocity components. Superscript '+' indicates the normalisation using viscous length and velocity scales which are ν/U_τ and U_τ respectively, where ν is the kinematic viscosity and U_τ is the friction velocity.

EXPERIMENTAL SETUP

The low Reynolds number experiments are conducted in the open return turbulent boundary layer wind tunnel at The University of Melbourne (the 'GWT'). The facility is a zero pressure gradient (ZPG) tunnel with a test section volume of $6.7 \times 0.94 \times 0.38 \text{ m}^3$. The higher Reynolds number experiments are conducted in the High Reynolds number boundary layer wind tunnel (HRNBLWT). Further details of each experiment are provided in table 1. Here we define the boundary layer thickness, δ as the wall-normal distance where the mean velocity achieves 99 % of the freestream velocity. Further, the friction velocity, U_τ , is obtained by a Clauser chart method using the log law constants, $\kappa = 0.4$ and $A = 5$.

The low Reynolds number experimental technique employs two single-wire hot-wire probes: HW1 and HW2 (as shown in figure). The length (l) and diameter (d) of the hot-wire sensors are $500\mu\text{m}$ and $2.5\mu\text{m}$ respectively to maintain an l/d ratio of 200 and $l^+ \approx 17$. The hot-wires are operated using an in-house Melbourne University constant temperature anemometer (MUCTA). For sufficiently converged statistics, the hot-wire velocity measurements are recorded for 32000 boundary layer turnover times (TU_∞/δ).

Facility	U_∞ (m/s)	δ (m)	U_τ (m/s)	Re_τ	z^+
GWT	15	0.056	0.545	1950	100
GWT	15	0.056	0.545	1950	200
HRNBLWT	40	0.337	1.231	26090	418

Table 1. Details of experimental data.

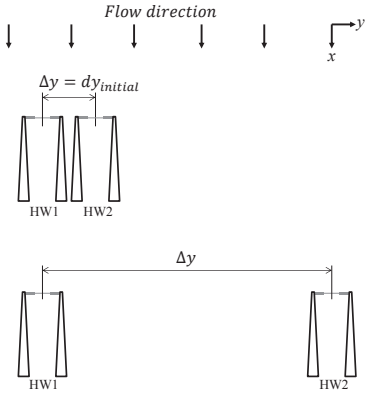


Figure 1. Schematic of the arrangement of hot-wires to measure the spanwise correlation in the low Reynolds number GWT.

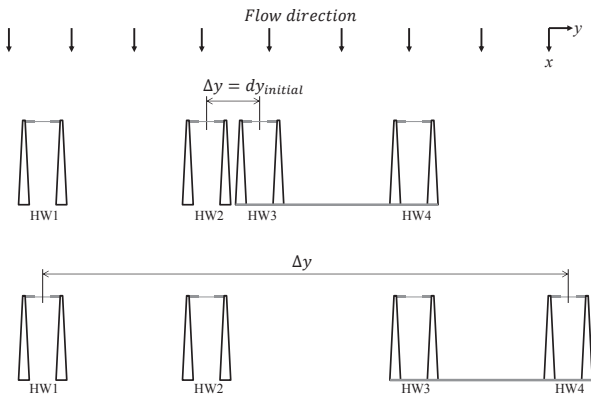


Figure 2. Schematic of the arrangement of hot-wires to measure the spanwise correlation in the high Reynolds number HRNBLWT.

Both hot-wires are calibrated immediately before and after each measurement to allow correction for drift in the hot-wire voltage during the experiment. HW1 is calibrated in the freestream with respect to the known mean velocities obtained with a Pitot-static probe. Since the arrangement did not allow HW2 to move to the freestream, calibration information from HW1 is used to calibrate HW2, while placed inside the boundary layer. This is achieved by placing both wires at the same wall-normal location. Since this calibration is carried out inside the turbulent boundary layer, the sampling time is increased compared to the freestream calibrations to ensure the convergence of mean velocity.

At the start of the measurement, HW1 and HW2 are positioned close to each other, at a fixed wall-normal location, as shown in figure . $dy_{initial}$ corresponds to the initial centre to centre spacing between the hot-wire sensors. For the present measurements, both HW1 and HW2 are sampled simultaneously, with HW1 at a fixed position, while HW2 is traversed in the spanwise direction upto a final spacing of $\Delta y \sim 3.5\delta$ (see figure). To acquire spatial information at smaller spanwise distances the spanwise traversing mechanism of HW2 is traversed on a logarithmic scale.

For the higher Reynolds number experiment, a similar system is employed, however, there are two stationary wires and two traversing wires (see figure 2) to halve the duration of an experi-

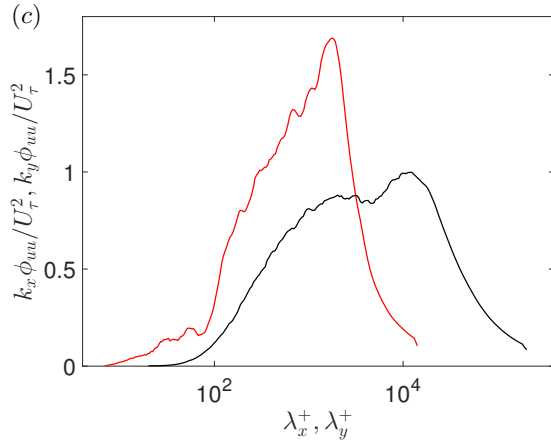
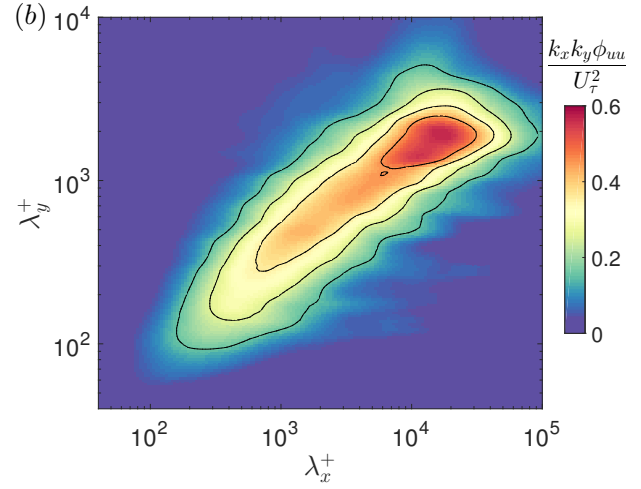


Figure 3. (a) Normalised 2-D correlation constructed from the velocity time series, (b) 2-D spectra obtained from the 2-D correlation and (c) 1-D streamwise (—) and 1-D spanwise (- -) spectra obtained by integrating the 2-D spectra.

ment and halve the required spanwise traversing length. This was necessary owing to physical limitations regarding the infrastructure of the wind-tunnel. The experimental method is identical, but with HW1 and HW2 traversing together in the spanwise direction, while HW3 and HW4 are fixed in position.

CALCULATING 2D SPECTRA FROM SINGLE POINT HOT-WIRE DATA

The velocity time-series of any pair of hot-wires separated by a spanwise distance Δy can be used to calculate the two-dimensional two-point correlation if Taylor's frozen turbulence hypothesis is invoked to convert the temporal data to spatial. The local mean velocity, U , is used as the convection velocity such that the streamwise spacing between data points is $\Delta x = U\Delta t$, where Δt is the sampling period of the hot-wire signal. By traversing wires in the spanwise direction (i.e. for a range of Δy) we can obtain the full 2D two-point correlation of streamwise velocity,

$$R_{uu}(\Delta x, \Delta y) = \overline{u_1(x, y)u_2(x + \Delta x, y + \Delta y)}. \quad (1)$$

Figure 3(a) shows an example of the 2-D correlation normalized by the variance of the velocity time series.

A 2-D Fourier transformation of the computed 2-D correlation yields the 2-D spectrum of streamwise velocity fluctuations as a

function of streamwise and spanwise wavenumbers, k_x and k_y ,

$$\phi_{uu}(k_x, k_y) = \int \int_{-\infty}^{\infty} R_{uu}(\Delta x, \Delta y) e^{-j2\pi(k_x \Delta x + k_y \Delta y)} d(\Delta x) d(\Delta y). \quad (2)$$

Here j is a unit imaginary number. Figure 3(b) shows the 2-D energy spectrum of streamwise velocity fluctuations calculated using the above procedure (note that wavelengths, λ_x and λ_y are used in this figure for ease of interpretation). The one-dimensional spectra for a specified streamwise wavelength can be calculated by simply integrating the 2-D spectra across all spanwise wavelengths for that streamwise wavelength and vice-versa for the 1-D spectra for a specified spanwise wavelength. Figure 3(c) shows the 1-D spectra of u as a function of streamwise and spanwise wavelengths obtained from the 2-D spectrum (shown in figure 3(b)). The area under the 1-D streamwise and spanwise spectra is equivalent to the variance of the streamwise velocity at that wall-normal location.

The results obtained from the experiments are validated against the DNS of ZPG boundary layer data of Sillero *et al.* (2014). The same technique described above is employed using the DNS data to first calculate the 2-D two-point correlation map and then apply a Fourier transform to determine the 2-D spectra (even though the 2-D spectra can be calculated directly). In other words, we simulate the hot-wire experiment using the DNS velocity fields. By selecting streamwise velocity traces at the same spanwise spacing as in the experiment, the effect of hot-wire minimum spacing and chosen spacings during the experiment can be checked (at least for the low Reynolds number case). Figure 4 shows a comparison between a contour of constant energy from the 2-D spectra, at $k_x k_y \phi_{uu} / U_\tau^2 = 0.15$, from both experiments and DNS.

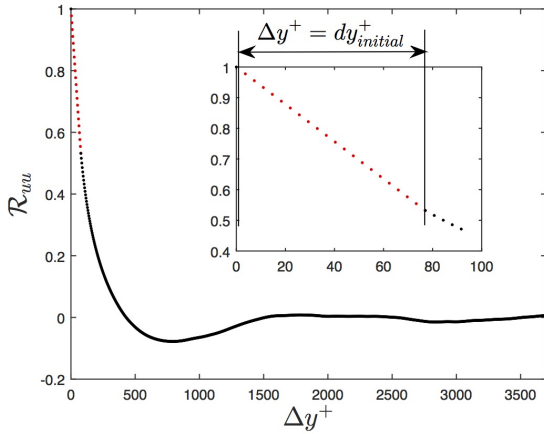


Figure 5. 1-D spanwise correlation using truncated DNS data with correlation values for $\Delta y < dy_{initial}$ linearly interpolated.

The results show good agreement between the experimental (\dots) and DNS (---) results at $z^+ \approx 200$ (figure 4b), however, closer to the wall ($z^+ \approx 100$) a larger disagreement in the small scale region is present (figure 4a) due to the finite initial spacing ($dy_{initial}$) between the hot-wires (see figure). Ideally, $dy_{initial}^+$ should be sufficiently small so that the smallest scales are well resolved. However, for the present experimental technique, it is not physically possible to reduce $dy_{initial}^+$ below a limit where the two hot-wires come into contact with each other. The minimum hot-wire spacing means that there are no two-point correlation values for $\Delta y = 0 - dy_{initial}$;

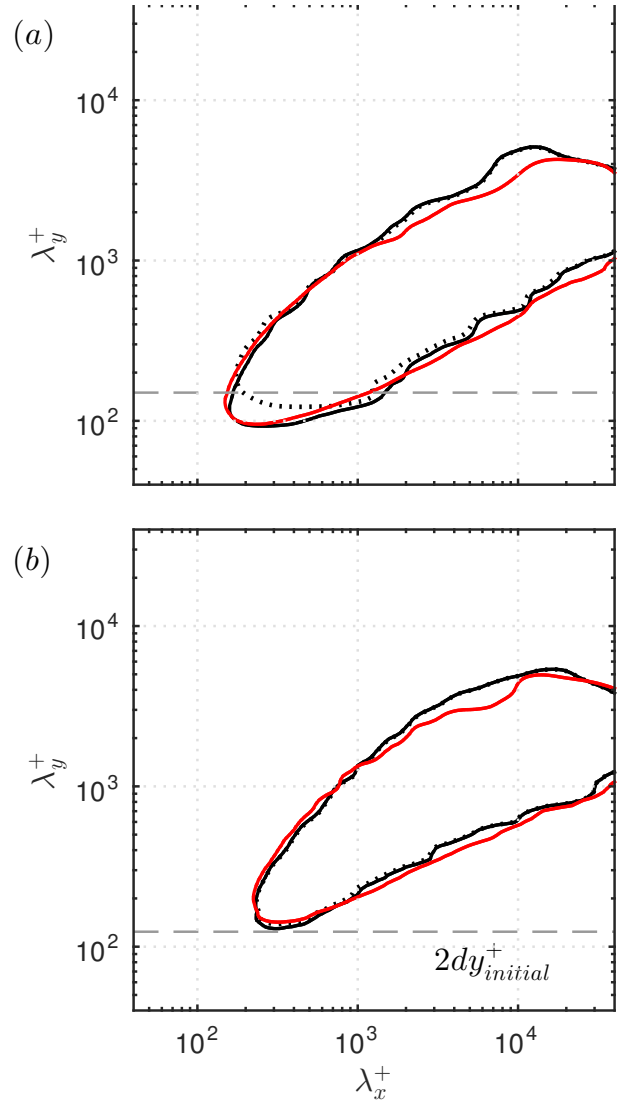


Figure 4. Comparison of experimental and DNS results for $k_x k_y \phi_{uu} / U_\tau^2 = 0.15$ at $Re_\tau \approx 2000$ and, (a) $z^+ \approx 100$ and (b) $z^+ \approx 200$; where, \dots uncorrected experiment; --- corrected experiment and --- DNS

these correlation values are needed are obtained by simple linear interpolation, meaning the small-scale energy spectra is incorrect. The affected region of the 2-D spectra diminishes for large wall-distance since the smallest energetic scales increase in size with distance from the wall. Because the area under the 2-D spectra is equal to the variance of the velocity, unresolved small-scale energy is redistributed throughout the spectrum – even to the larger scales. Using the DNS data, we can determine a correction to the 2-D spectra as outlined below.

The first step is to calculate the two-point correlation of velocity using DNS data with minimum spanwise spacing equivalent to $dy_{initial}$ following the experiment. The missing two-point correlation values between $\Delta y = 0 - dy_{initial}$ are linearly interpolated in the same way as done for the experiment. This is illustrated for $\Delta x = 0$ in figure 5. The 2-D spectra is then calculated with the small-scale interpolated 2-D two-point correlation of streamwise velocity. The result is shown in figure (b) and can be easily compared with the true 2-D spectra shown in figure (a). Figure 5 shows the 1-D correlation in the spanwise direction obtained using DNS data.

The difference ($\Delta k_x k_y \phi_{uu}^+$) of the interpolated and original 2-D

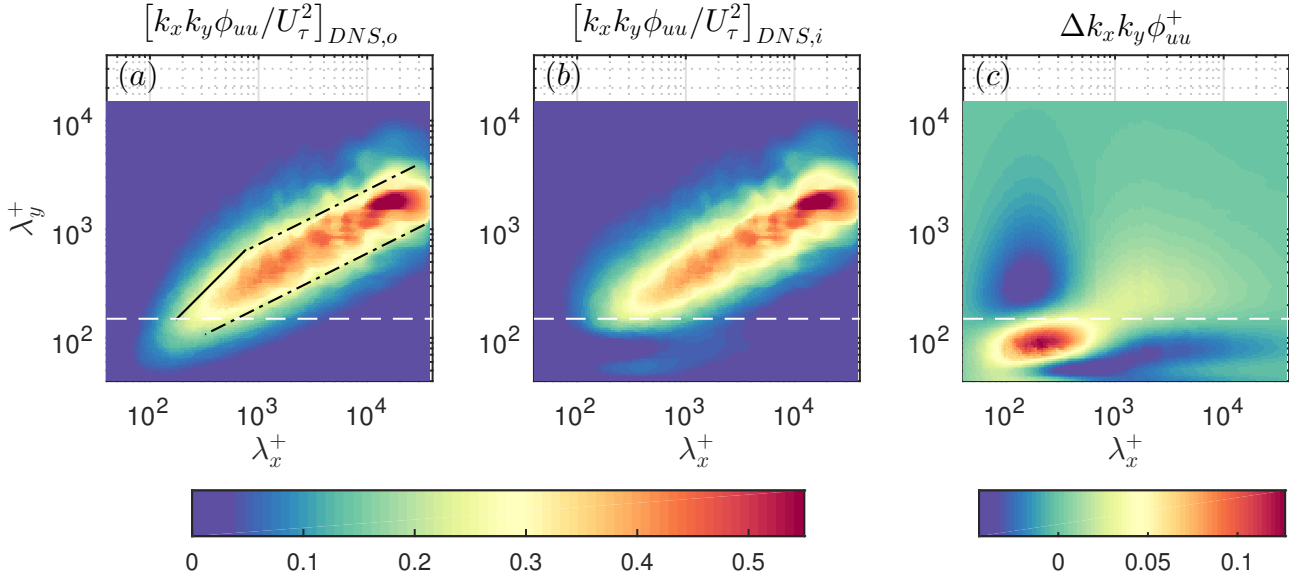


Figure 6. (a) 2-D spectra obtained from the original DNS correlation, where — and - - represent the relationships $\lambda_y/z \sim \lambda_x/z$ and $\lambda_y/z \sim (\lambda_x/z)^{1/2}$ respectively as reported by Del Alamo *et al.* ?, (b) 2-D spectra obtained from the interpolated DNS correlation and (c) difference between (a) and (b).

spectra is computed and shown in figure (c). This difference corresponds to the amount of energy redistributed due to $dy_{initial}^+$. This difference can be added to the experimental data to give the corrected 2-D spectra. Namely,

$$\Delta k_x k_y \phi_{uu}^+ = \left[\frac{k_x k_y \phi_{uu}}{U_\tau^2} \right]_{DNS,o} - \left[\frac{k_x k_y \phi_{uu}}{U_\tau^2} \right]_{DNS,i} \quad (3)$$

$$\left[\frac{k_x k_y \phi_{uu}}{U_\tau^2} \right]_{EXP,c} = \left[\frac{k_x k_y \phi_{uu}}{U_\tau^2} \right]_{EXP} + \Delta k_x k_y \phi_{uu}^+ \quad (4)$$

where the subscripts DNS,o and DNS,i represent original and interpolated DNS results respectively. Similarly, EXP,c and EXP represents the corrected and uncorrected experimental results respectively.

Figure (c) shows that the differences due to the minimum spacing is largest near λ_y^+ corresponding to $dy_{initial}^+$ (see white dashed line in figure), as expected. However, it is also evident that the difference is not limited to small scales and is, in fact, spread over a large range of wavelengths. The correction is effective on the hot-wire data and an example is shown in figure 4, where a contour of constant energy from the corrected experimental spectrum (—) is compared against the DNS (—) as shown in figure 4. Much better agreement with DNS is observed at smaller scales compared with the uncorrected experimental spectrum (···). It is also evident that the correction is minimal at the larger wall-distance.

The correction method determined with low Reynolds number DNS data is expected to be valid at higher Reynolds numbers since inner-scaled energy contributions from small scales are Reynolds number invariant (Hutchins *et al.*, 2009). Therefore, this correction is applied to all the experimental data presented in this paper for completeness; however, no conclusions drawn in the following are dependent on the effects of the correction scheme.

2-D SPECTRA FOR LOW AND HIGH Re

Figure 7 shows the experimentally determined 2-D spectra for low and high Reynolds numbers at the base of the logarithmic region $2.6\sqrt{Re_\tau}$, corresponding to $z^+ = 100$ and 420, respectively. The low Reynolds number data follow the same trends as ?, namely,

the energetic ridge of the spectra follows a $\lambda_y/z \propto \lambda_x/z^{0.5}$ behaviour. This is problematic from a classical viewpoint, because such a scaling discounts self-similarity of the large-scales. Self-similarity of the inertial (large) scales is fundamental to many turbulence models and various hypotheses, for example, the attached eddy hypothesis. However, the high Reynolds number data show a surprisingly different trend in the largest scales. There appears to be a shift in the high-energy contours back toward the $\lambda_y \propto \lambda_x$ behaviour expected of self-similar large-scales. This result suggests that self-similarity becomes evident at very high Reynolds numbers only.

ATTACHED EDDY MODELLING

Townsend's attached eddy hypothesis formed the basis of the Perry & Chong (1982) Attached Eddy Model. One of the tenets of the hypothesis is that the energy containing motions in the logarithmic region are self-similar. That is, their energy per unit area is constant and their lengths scales follow a geometric progression. Given the above observation that the largest-scales show self-similar behaviour at high Reynolds number, we here utilise the attached eddy model to check the expected trends of the spectrum for a purely self-similar flow structure. In this exercise, hierarchies of representative eddies are used to model the dominant energy contributions in the turbulent boundary layer. The modelling follows the procedure given in Perry *et al.* (Perry *et al.*, 1986), however, here we will consider 3 types of representative structures: *i.* A single hairpin-shaped eddy as in Perry *et al.*; *ii.* a packet of hairpin-shaped eddies with length to width ratio ~ 3 and; *iii.* a packet of hairpin-shaped eddies with length to width ratio ~ 6 designed to match the ratio of aspect ratio of the highly energetic ridge evident in figure 7(b). Schematics of the representative eddies and a slice through the velocity field at 0.2 times the largest eddy height are shown in figure 8. The resulting 2-D spectra from these simulations is shown in figure 9. For comparison, the figure includes the same red guidelines from figure 7(b) showing square-root (red dashed) and linear (red solid) relationships between widths and lengths of eddies that described the experimental data. It is clear that the single self-similar eddies do not describe the experimental 2-D spectra very well and that the

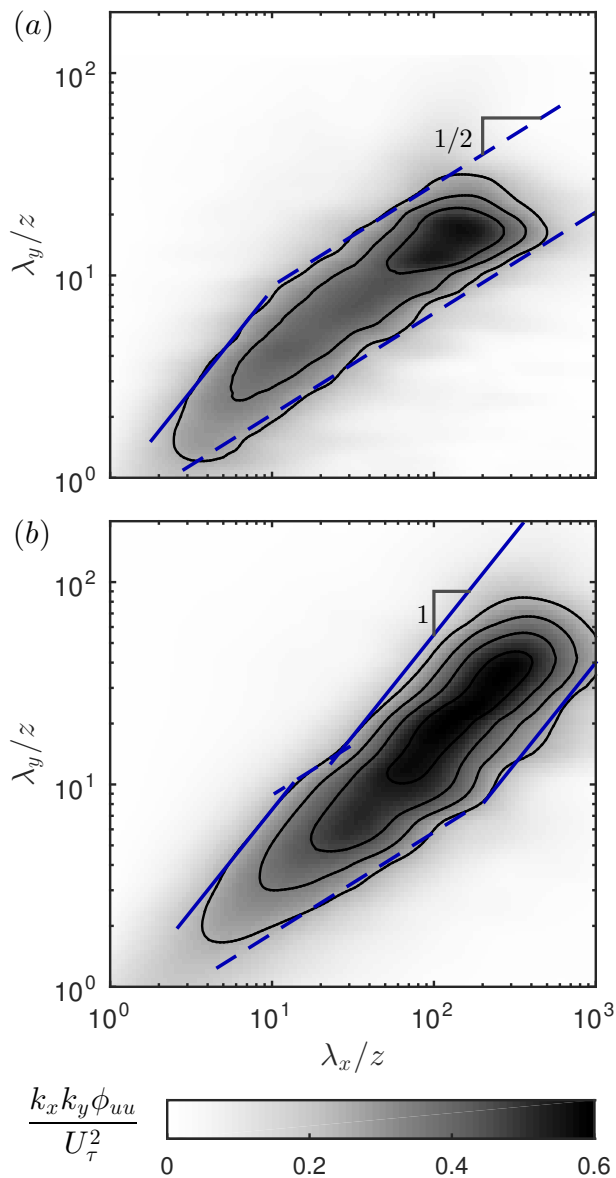


Figure 7. 2-D spectra of streamwise velocity at $2.6\sqrt{Re_\tau}$ for (a) Low Reynolds number ($Re_\tau \approx 2000$) and (b) High Reynolds number ($Re_\tau \approx 26000$). Blue solid lines indicate $\lambda_y \propto \lambda_x$, blue dashed lines indicate $\lambda_y/z \propto \sqrt{\lambda_x/z}$

higher aspect ratio (longer packets) provide a superior match to the experimental data. Interestingly, the spread of energy across spanwise wavelengths for a given streamwise wavelengths is qualitatively similar to the experimental data, even though only one representative eddy is used in the simulation. This is possibly only due to the fact that eddy velocity signatures are not truly sinusoidal in either the streamwise or spanwise directions.

CONCLUSION

Two-dimensional spectra of the streamwise velocity component for low and very high Reynolds number ($Re_\tau = 26000$) are measured in a wind-tunnel boundary layer. The low Reynolds number data agree very well with DNS studies, in particular with the 2D spectra documented in del Álamo *et al.* (2004). At much higher Reynolds numbers, we observe a distinct change in behaviour of the large-scale energy: the contours of 2-D spectra for small scales follow a similar behaviour to the low Reynolds number case, how-

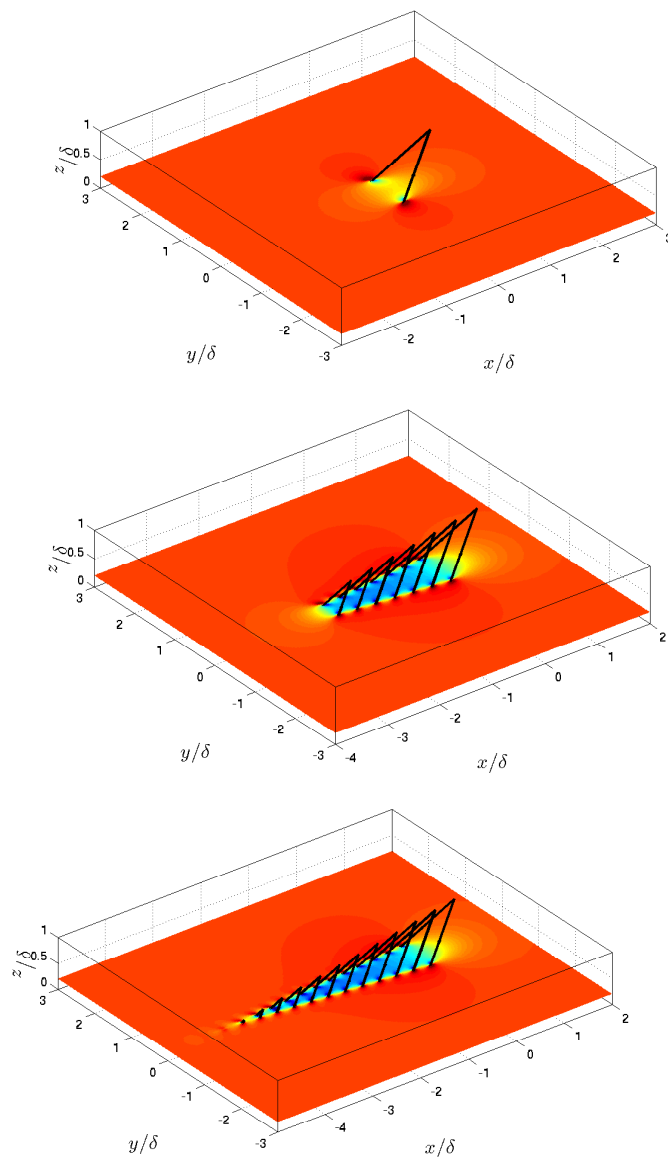


Figure 8. Schematics of the representative eddies used in attached eddy modelling. The contours show qualitatively the velocity field near the base of the eddies. Three simulations were conducted with a single eddy (top), a small packet (middle) and a large packet (bottom).

ever, the large streamwise and spanwise wavelengths (λ_x and λ_y) are observed to tend towards a $\lambda_y \sim \lambda_x$ relationship. Where many previous have not found evidence for self-similarity, these new high Reynolds number data provide some confidence that self-similarity at practically high Reynolds numbers will exist.

The attached eddy model of Perry & Chong is used for comparison with the experimental data. It is shown that by choosing an appropriate grouping (packet) of representative eddies, the dominant trends of the high Reynolds number 2D spectra can be reproduced from a model that relies on the self-similarity of large-scale vortical structures.

REFERENCES

- del Álamo, J. C., Jiménez, J., Zandonade, P. & Moser, R. D. 2004 Scaling of the energy spectra of turbulent channels. *J. Fluid Mech.* **500**, 135–144.
- Chung, D., Marusic, I., Monty, J. P., Vallikivi, M. & Smits, A. J.

2015 On the universality of inertial energy in the log layer of turbulent boundary layer and pipe flows. *Exp. Fluids* **56**, 1–10.

Davidson, P. A., Nickels, T. B. & Krogstad, P. Å. 2006 The logarithmic structure function law in wall-layer turbulence. *J. Fluid Mech.* **550**, 51–60.

Hutchins, N., Nickels, T. B., Marusic, I. & Chong, M. S. 2009 Hot-wire spatial resolution issues in wall-bounded turbulence. *J. Fluid Mech.* **635**, 103–136.

Nickels, T. B., Marusic, I., Hafez, S. & Chong, M. S. 2005 Evidence of the k_1^{-1} law in a high-Reynolds-number turbulent boundary layer. *Phys. Rev. Lett.* **95**, 074501.

Perry, A. E. & Chong, M. S. 1982 On the mechanism of wall turbulence. *J. Fluid Mech.* **119**, 173–217.

Perry, A. E., Henbest, S. & Chong, M. S. 1986 A theoretical and experimental study of wall turbulence. *J. Fluid Mech.* **165**, 163–199.

Rosenberg, B. J., Hultmark, M., Vallikivi, M., Bailey, S. C. C. & Smits, A. J. 2013 Turbulence spectra in smooth-and rough-wall pipe flow at extreme Reynolds numbers. *J. Fluid Mech.* **731**, 46–63.

Sillero, J. A., Jiménez, J. & Moser, R. D. 2014 Two-point statistics for turbulent boundary layers and channels at Reynolds numbers up to $\delta^+ \approx 2000$. *Phys. Fluids* **26**, 105109.

Townsend, A. A. 1976 *The structure of turbulent shear flow*, 2nd edn. Cambridge university press.

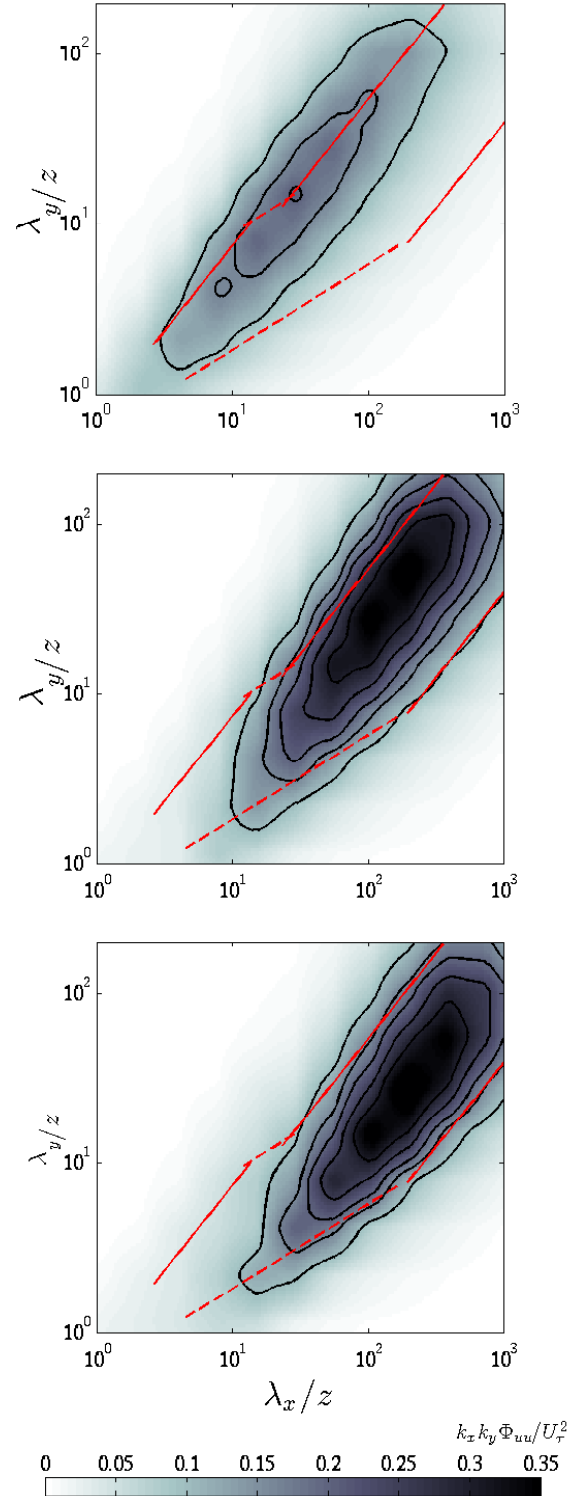


Figure 9. Attached eddy modelling: 2-D spectra of streamwise velocity at $2.6\sqrt{Re_\tau}$ for (a) single representative eddy, (b) packets of eddies with aspect ratio (length to width) ~ 3 and (c) packets of eddies with aspect ratio (length to width) ~ 6 . $Re_\tau \approx 26000$ for the model. Solid and dashed lines as in figure 7.